Commun. Comput. Chem.
doi: 10.4208/cicc.2013.v1.n3.1

Vol.**1**, No.**3**, pp.205-215
August 2013

COMMUNICATION

Effects of Different-type Intermolecular Hydrogen Bonds on the Geometrical and Spectral Properties of 6-aminocoumarin Clusters in Solution

Dapeng Yang[a,1], Yonggang Yang[b], Yufang Liu[b]

[a]*Physics Laboratory, North China University of Water Resources and Electric Power, Zhengzhou 450045, PR China*

[b]*Department of Physics, Henan Normal University, Xinxiang 453007, PR China*

Received 18 June 2013; Accepted (in revised version) 10 July 2013

Abstract: Geometrical and spectral properties of the hydrogen-bonded clusters formed by 6-aminocoumarin (6AC) with solvents of different hydrogen-bonding abilities have been investigated at CPCM-PBE0/6-311++G(d, p) theory level. Upon photo-excitation, type hydrogen bonds will be weakened whereas hydrogen bonds of B and C types should be strengthened. The weakening of hydrogen bond A is responsible for the blue-shifts of the absorption spectra in HFIP and TFE while strengthening of hydrogen bonds B_1 and B_2 are reasons for the red-shifts of the absorption spectra in DMSO. The absorption spectra of cluster 6AC-$(H_2O)_3$ is in better agreement with the experimental result than 6AC-$(H_2O)_5$.

AMS subject classifications: 74E40, 78M50

Keywords: 6-aminocoumarin clusters Hydrogen bonds of different types, Hydrogen bonding strengthening and weakening, Spectral red- and blue-shifts.

1. Introduction

Recently, important results on many properties of intermolecular hydrogen bonds, including their structures, energy changes upon electronic excitation as well as their impacts on the

---

[*] Corresponding author *E-mail address*: dpyang_ncwu@163.com. Tel: +86-371-13803712920.

spectral and photophysical properties of hydrogen-bonded chromophore molecules can be found in a number of theoretical [1-12] and experimental [13-24] works. Some TDDFT calculations have been performed to examine the relationship between the absorption spectra of 7-aminocoumarin and the formation of hydrogen bonds [3-5]. Using DFT and TDDFT methods, Zhao and Han [6] have demonstrated that the strengthening of the intermolecular hydrogen bonds upon photoexcitation can lower the excitation energy of a related excited state and induce an electronic spectral redshift, while the excited-state hydrogen bond weakening can heighten the excitation energy of a related excited state and induce an electronic spectral blueshift. Moreover, hydrogen bond formation and its effects on the absorption and fluorescence spectra of coumarins molecules are also the subjects of experimental works [14-17].

Krystkowiak and coworkers [25-26] have measured the absorption spectra of 6-aminocoumarin (6AC) in 1,1,1,3,3,3-hexafluoroisopropanol (HFIP), 2,2,2-trifluoroethanol (TFE), dimethylsulfoxide (DMSO) and water and compared with those in 1-chloro-n-propane (1-C_3H_7Cl). They concluded that the unusual blue- and red-shifts of absorption spectra of 6AC in solvents HFIP (TFE) and DMSO should be due to the weakening of hydrogen bond N…H-O (A type) and strengthening of hydrogen bonds N-H…O (C type) as a result of the excitation. In addition, they suggested the solute-solvent complexes made by all possible hydrogen bonds, that is 6AC-$(HFIP)_3$, 6AC-$(TFE)_3$, 6AC-$(DMSO)_2$ and 6AC-$(H_2O)_5$. However, as pointed out by Krystkowiak in the Introduction of Ref. 26, only theoretical calculations permit determinations of the geometrical structures of the hydrogen-bonded clusters and energies of the individual hydrogen bond formed in the clusters.

Table 1: The Kamlet and Taft (K-T) parameters (α,β) and the dielectric constant ε of the solvents.

Solvent	α	β	ε
1-C_3H_7Cl	0.00	0.00	8.59
HFIP	1.97	0.00	16.62
TFE	1.51	0.00	26.67
DMSO	0.00	0.76	46.45
H_2O	1.17	0.47	78.00

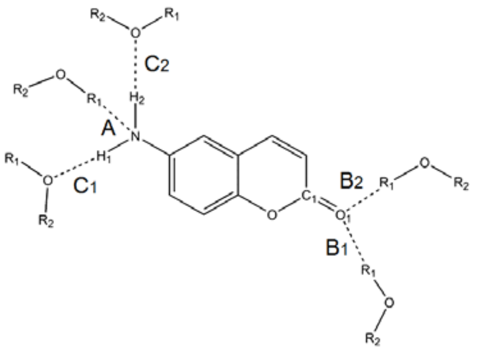

Figure 1: Illustration of three types of intermolecular hydrogen bonds formed between 6-aminocoumarin (6AC) and solvents.

6AC shows a simple structure as the 1,2-benzopyrone moiety is substituted by donor

-NH_2 and acceptor -C=O groups along the same molecule axis. To the best of our knowledge, there has been no theoretical calculation of both the geometric structures and the hydrogen bonding energies for this molecule and its hydrogen-bonded clusters up to now. Therefore, in the present paper, we carry out a detailed theoretical investigation (at the CPCM-PBE0/6-311++G(d, p) level of theory [27-35] using the Gaussian 09 program suite [36]) on the geometric structures and spectral properties of the various multiply hydrogen-bonded 6AC clusters formed with three HFIP molecules, three TFE molecules, two DMSO molecules and different numbers of water molecules, whose Kamlet-Taft parameters are listed in Table 1 [37, 38]. The K-T parameters α and β of a solvent characterize the ability of the solvent molecule to donate and accept a hydrogen atom from a solute molecule to form hydrogen bonds, respectively. The formations of the hydrogen-bonded clusters between 6AC and different solvent molecules are illustrated in Figure 1 and they are named as 6AC-$(HFIP)_3$, 6AC-$(TFE)_3$, 6AC-$(DMSO)_2$ and 6AC-$(H_2O)_n$ (n=2, 3, 4, 5), respectively. Special attentions are paid to the possible changes of each type of hydrogen bonds formed in the clusters going from the ground state S_0 to the first excited singlet state S_1 as well as its effects on the properties of the absorption spectra of the 6AC molecule.

2. Results and Discussions

2.1 Ground-State Geometric Structures

The ground-state geometric conformations of the various multiply hydrogen-bonded 6AC clusters 6AC-$(HFIP)_3$, 6AC-$(TFE)_3$, 6AC-$(DMSO)_2$ and 6AC-$(H_2O)_n$ (n=2, 3, 4, 5) are composed and fully optimized at the CPCM-PBE0/6-311++G(d, p) level of theory and shown in **Figure 2**. The hydrogen bond lengths and corresponding bonding energies are listed in **Table 2**. In cluster 6AC-$(HFIP)_3$, three HFIP molecules are hydrogen-bonded to the 6AC molecule through hydrogen bonds A, B_1 and B_2, whose bond lengths (bond energies) are 1.781 Å (2719 cm^{-1}), 1.755 Å (2485 cm^{-1}) and 1.781 Å (2354 cm^{-1}) respectively, see **Figure 2a**., which indicates that hydrogen bond A is much stronger than hydrogen bonds B_1 and B_2 in the ground state. Similarly, in cluster 6AC-$(TFE)_3$, three TFE molecules are hydrogen-bonded to 6AC molecule through hydrogen bonds A, B_1 and B_2, whose bond lengths (bond energies) are 1.842 Å (1558 cm^{-1}), 1.783 Å (2049 cm^{-1}) and 1.778 Å (2021 cm^{-1}) respectively, see **Figure 2a**. Compared with their corresponding ones in cluster 6AC-$(HFIP)_3$, the three hydrogen bonds formed in cluster 6AC-$(TFE)_3$ are all a little weaker, which should be due to the smaller α value of TFE than HFIP. In cluster 6AC-$(DMSO)_2$, two DMSO molecules are hydrogen-bonded to 6AC molecule through hydrogen bonds C_1 and C_2, whose bond lengths (bond energies) are 1.921 Å (2852 cm^{-1}) and 1.946 Å (2362 cm^{-1}) respectively, also see **Figure**

2a.

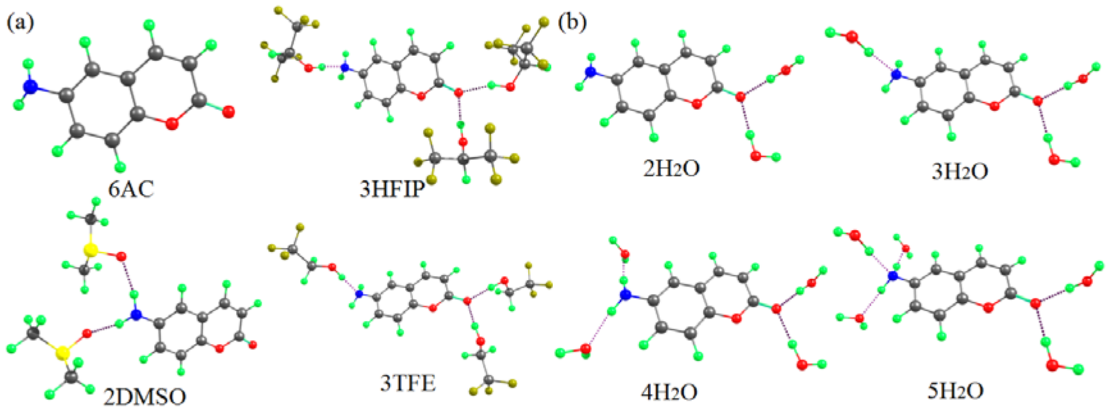

Figure 2: Optimized structures of (a) 6AC monomer and hydrogen-bonded 6AC clusters formed with three HFIP molecules, three TFE molecules and two DMSO molecules and (b) clusters formed with 2, 3, 4 and 5 water molecules.

Krystkowiak and coworkers [26] have suggested that five water molecules should participate in the formation of the cluster, namely 6AC-$(H_2O)_5$. In the present work, for reasons that will be elucidated in Section 2.2, the 6AC-$(H_2O)_n$ clusters with two (B_1 and B_2), three (A, B_1 and B_2), four (B_1, B_2, C_1 and C_2) and five (A, B_1, B_2, C_1 and C_2) water molecules are all optimized and presented in **Figure 2b**. In cluster 6AC-$(H_2O)_2$, two water molecules are hydrogen-bonded to 6AC molecule through hydrogen bonds B_1 and B_2, whose bond lengths (bonding energies) are 1.855 Å (2013 cm^{-1}) and 1.850 (1907 cm^{-1}) Å respectively, see **Figure 2b**, the left upper one. When a third water molecule is added to cluster 6AC-$(H_2O)_2$ through hydrogen bond A, cluster 6AC-$(H_2O)_3$ is formed, see **Figure 2b**, the right upper one. The bond length of hydrogen bond A in cluster 6AC-$(H_2O)_3$ is 1.930 Å, whose bonding energy is 1310 cm^{-1}, and those of hydrogen bonds B_1 and B_2 are similar to their corresponding ones in cluster 6AC-$(H_2O)_2$. When another two water molecules are added to cluster 6AC-$(H_2O)_2$ through hydrogen bonds C_1 and C_2, we get cluster 6AC-$(H_2O)_4$, see **Figure 2b**, the left bottom one. The bond lengths (bonding energies) of hydrogen bonds C_1 and C_2 in cluster 6AC-$(H_2O)_4$ are 2.004 Å (1558 cm^{-1}) and 2.002 Å (1552 cm^{-1}) respectively. When all the three types of hydrogen bonds are formed by five water molecules and 6AC molecule, we get the cluster 6AC-$(H_2O)_5$, as suggested by Krystkowiak and coworkers [26]. In cluster 6AC-$(H_2O)_5$, hydrogen bonds of both types A and C are stronger than their corresponding ones in clusters 6AC-$(H_2O)_3$ and 6AC-$(H_2O)_4$ respectively. Moreover, the strength of hydrogen bonds B_1 and B_2 in this cluster is similar to that in other 6AC-$(H_2O)_n$ clusters. For clusters 6AC-$(HFIP)_3$, 6AC-$(TFE)_3$ and 6AC-$(H_2O)_3$, hydrogen bonds of both types A and B formed in 6AC-$(HFIP)_3$ are strongest while those formed in 6AC-$(H_2O)_3$ are the weakest and those formed in 6AC-(TFE)$_3$ lie between them. The two hydrogen bonds of type C formed in cluster 6AC-(H$_2$O)$_4$ are weaker than those formed in 6AC-(DMSO)$_2$. Therefore, it can be concluded that the strength of the various types of hydrogen bonds is related to the K-T parameters of the solvents.

Table 2: Hydrogen bond lengths (Å) and bonding energies (cm^{-1}, in the parentheses) calculated at CPCM-PBE0/6-311++G(d, p) level of theory.

	3HFIP	3TFE	2DMSO	2H$_2$O	3H$_2$O	4H$_2$O	5H$_2$O
A	1.781	1.842			1.930		1.895
	(2719)	(1558)			(1310)		(1801)
B$_1$	1.755	1.783		1.855	1.861	1.849	1.854
	(2485)	(2049)		(2013)	(1949)	(2178)	(2090)
B$_2$	1.781	1.778		1.850	1.856	1.843	1.849
	(2354)	(2021)		(1907)	(1852)	(2102)	(2045)
C$_1$			1.931			2.004	1.984
			(2852)			(1558)	(1736)
C$_2$			1.946			2.002	1.986
			(2362)			(1552)	(1744)

2.2 Electronic Excitation Energies and Frontier MOs

The electronic excitation energies and corresponding oscillation strengths of the S$_1$ states for both the 6Ac monomer (in 1-C$_3$H$_7$Cl) and its various multiply hydrogen-bonded clusters are calculated at the TD-CPCM-PBE0/6-311++G(d, p) level of theory and presented in **Table 3.** The experimental absorption spectra maxima of 6AC in corresponding solvents obtained by Krystkowiak [26] are also listed in **Table 3** for comparisons. From **Table 3**, it can be found that for 6AC monomer, the S$_1$-state excitation energy is calculated to be 366.73 nm with 1-C$_3$H$_7$Cl as the solvent, which is exactly the same as that obtained by Krystkowiak in solvent 1-C$_3$H$_7$Cl [26]. From 6AC monomer to clusters 6AC-(HFIP)$_3$ and 6AC-(TFE)$_3$, the calculated excitation energies are blue-shifted to 344.05 and 348.50 nm with the oscillator strengths increased from 0.0868 to 0.0937 and 0.0896, respectively. The calculated S$_1$-state excitation energies are once again in good agreement with the experimental absorption spectra maxima (338.98 and 346.98 nm for 6AC in solvents HFIP and TFE respectively [26]), which has demonstrated the reasonableness of the composed cluster conformations for 6AC-(HFIP)$_3$ and 6AC-(TFE)$_3$. Contrary to the situations of clusters 6AC-(HFIP)$_3$ and 6AC-(TFE)$_3$, the calculated excitation energy of cluster 6AC-(DMSO)$_2$ is red-shifted to 399.96 nm from 6AC monomer and the oscillator strength is decreased to 0.073. The calculated

S_1-state excitation energy of cluster 6AC-$(DMSO)_2$ is 14 nm larger than the experimental result (385.95 nm in DMSO [26]), and both of them are red-shifted compared with that of 6AC monomer. For the four clusters formed by 6AC with two, three, four and five water molecules, the calculated S_1-state excitation energies are 379.05, 352.97, 408.29 and 373.02 nm respectively, with oscillator strengths 0.0770, 0.0897, 0.0677 and 0.0781. The absorption maximum wavelength of 6AC in water obtained by Krystkowiak and coworkers is 28090 cm^{-1} (356.00 nm) [26]. The calculated S_1-state excitation energy of cluster 6AC-$(H_2O)_3$ is just 3 nm larger than the experimental result. Therefore, in the ground state of 6AC molecule in water solution, most 6AC molecules should be hydrogen-bonded with three water molecules in the way of cluster 6AC-$(H_2O)_3$, see **Figure 2b**, the right upper one, which is not consistent with the assumption of Krystkowiak and coworkers [26].

Table 3: Calculated wavelengths $\lambda_{Abs.}^{\max}$ [nm] (frequency ν [10^3 cm^{-1}]), oscillator strength f and the major contribution (>50%) of the orbital transitions of the hydrogen-bonded 6AC clusters along with experimental results (Expt.) [26]. H: HOMO, L: LUMO.

	6AC	3HFIP	3TFE	2DMSO	$2H_2O$	$3H_2O$	$4H_2O$	$5H_2O$
$\lambda_{Abs.}^{\max}$	366.73	344.05	348.50	399.96	379.04	352.97	408.29	373.02
ν	27.27	29.06	28.69	25.00	26.38	28.33	24.49	26.81
f	0.0868	0.0937	0.0896	0.0730	0.0770	0.0897	0.0677	0.0781
H→L	98%	97%	97%	99%	98%	97%	99%	98%
Expt.	366.97 (27.25)	338.98 (29.50)	346.98 (28.82)	385.95 (25.91)	356.00 (28.09)			

The molecular orbitals (MOs) energy levels and shapes of the highest occupied molecular orbital (HOMO) and the lowest unoccupied molecular orbital (LUMO) are presented in **Figure 3**. **Figure 3a** shows the HOMO and LUMO energy levels as well as their energy differences. In contrast with 6AC monomer, the HOMO and LUMO energy levels of clusters 6AC-$(HFIP)_3$ and 6AC-$(TFE)_3$ are decreased, whereas the energy differences are increased to 0.1607 and 0.1589 eV respectively due to participation of hydrogen bond A. For cluster 6AC-$(DMSO)_2$, the HOMO and LUMO energy levels are increased, whereas the energy difference is decreased to 0.1417 eV compared with those of 6AC monomer due to formation of hydrogen bonds B_1 and B_2. As for the four clusters formed with 2, 3, 4 and 5 water molecules, their LUMO energy levels are similar to each other, whereas the HOMO energy level of cluster 6AC-$(H_2O)_3$ is most decreased and the energy difference is increased to 0.1573 eV. Furthermore, it can be noted from **Figure 3b** that the orbital transition from HOMO to LUMO involves an intramolecular charge redistribution from the N atom of the amine group to the rest part of the 6AC molecule, especially the carbonyl group of the 6AC moiety. Thus, the S_1 state of the 6AC monomer may be an intramolecular charge-transfer (ICT) state, whereas the S_1 state of hydrogen-bonded 6AC clusters should be the locally excited (LE) state on the 6AC moiety. Moreover, it can be inferred that the A type hydrogen bond should become weakened whereas hydrogen bonds of B and C types should become strengthened upon the photoexcitation of 6AC from ground state S_0 to excited state S_1. The weakening of hydrogen bond A and strengthening of hydrogen bonds B and C after electronic excitation will impose less and more stabilization effects on the excited-state energy level compared with those on the ground state, respectively. Therefore, the energy level differences between the two electronic states will be increased and decreased accordingly, which should be responsible for the blue- and red-shifts of the excitation energy. Therefore, the red- and blue-shifts of the absorption spectra of 6AC in the above-mentioned solvents should be due to the intermolecular hydrogen bonds of different types and numbers as well as their different changes after the electronic excitation of 6AC.

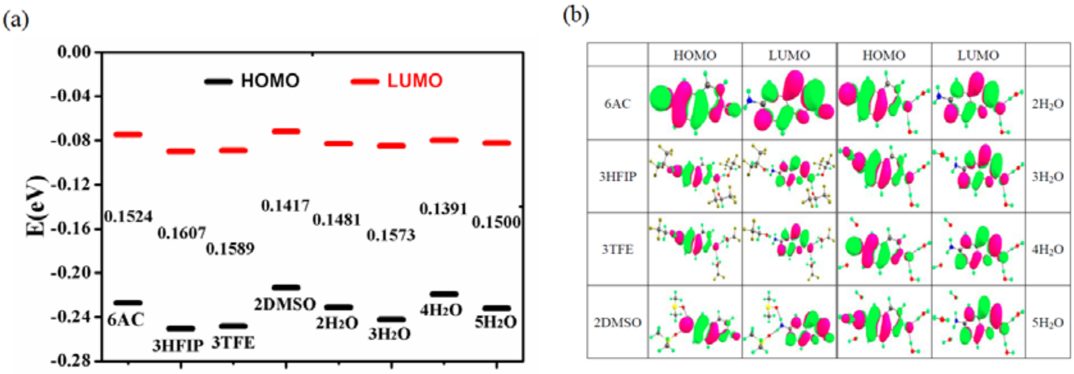

Figure 3: Calculated frontier molecular orbital (MO) energy levels (a) and shapes (b) of 6AC monomer and hydrogen-bonded 6AC clusters at the CPCM-TD-PBE0/6-311++G(d, p) level of theory.

3. Conclusions

The calculated S_1-state excitation energies for both the 6AC monomer (in 1-C_3H_7Cl) and its multiply hydrogen-bonded clusters at the CPCM-TD-PBE0/6-311++G(d, p) level of theory are all in good agreement with the experimental absorption spectra maxima. Due to the electron density redistribution from the amine group to the carbonyl group of the 6AC molecule upon photoexcitation, A type hydrogen bonds will be weakened whereas B and C types of hydrogen bonds will be strengthened compared with those in the ground state. The weakening and strengthening of the intermolecular hydrogen bonds should be responsible for the blue- and red-shifts of the absorption spectra. Further investigations, especially those on the geometric structures of the clusters in the first singlet excited state, will be carried out soon.

Acknowledgement

This work was supported by the National Natural Science Foundation of China (Grant No. 11274096), the China Postdoctoral Science Foundation Funded Project (Grant No. 2013M530951), the Innovation Scientists and Technicians Troop Construction Projects of Henan Province of China (Grant No. 124200510013) and the Science and Technology Research Key Project of Education Department of Henan Province of China (Grant No. 13A140690).

References

[1] G.-J. Zhao, J.-Y. Liu, L.-C. Zhou, K.-L. Han, Site-selective photoinduced electron transfer from alcoholic solvents to the chromophore facilitated by hydrogen bonding: A new fluorescence quenching mechanism, J. Phys. Chem. B, 111 (2007), 8940-8945.

[2] G.-J. Zhao, K.-L. Han, Ultrafast hydrogen bond strengthening of the photoexcited fluorenone in alcohols for facilitating the fluorescence quenching, J. Phys. Chem. A, 111 (2007), 9218-9223.

[3] W.-W. Zhao, L. Pan, W.-S. Bian, J.-P. Wang, Influence of solvent polarity and hydrogen bonding on the electronic transition of Coumarin 120: A TDDFT study ChemPhysChem, 9 (2008), 1593-1602.

[4] P.-W. Zhou, P. Song, J.-Y. Liu, K.-L. Han, G.-Z. He, Experimental and theoretical study of the rotational reorientation dynamics of 7-animocoumarin derivatives in polar solvents: hydrogen-bonding effects, Phys. Chem. Chem. Phys., 11 (2009), 9440-9449.

[5] Y.-F. Liu, J.-X. Ding, R.-Q. Liu, D.-H. Shi, J.-F. Sun, Revisiting the electronic excite-state hydrogen bonding dynamics of coumarin chromophore in alcohols: undoubtedly strengthened not cleaved, J. Photochem. Photobiol. A, 201 (2009), 203-207.

[6] G.-J. Zhao, K.-L. Han, Dynamic effects of hydrogen bonding on tuning photochemistry: concerted hydrogen bond strengthening and weakening, ChemPhysChem, 9 (2008), 1842-1846.

[7] Y.-H. Liu, G.-J. Zhao, G.-Y. Li, K.-L. Han, Fluorescence quenching phenomena facilitated by excited-state hydrogen bond strengthening for fluorenone derivatives in alcohols, J. Photochem. Photobio. A, 209 (2010), 181-185.

[8] G.-J. Zhao, K.-L. Han, Role of intramolecular and intermolecular hydrogen bonding in both singlet and triplet excited states of aminofluorenones on internal conversion, intersystem crossing, and twisted intramolecular charge transfer, J. Phys. Chem. A, 113 (2009), 14329-14335.

[9] G.-Y. Li, G.-J. Zhao, Y.-H. Liu, K.-L. Han, G.-Z. He, TD-DFT study on the sensing mechanism of a fluorescent chemosensor for fluoride: excited-state proton transfer, J. Comput. Chem., 31 (2010),

1759-1765.

[10] K.-L. Han, G.-J. Zhao, Hydrogen bonding and transfer in the excited state, ISBN: 978-0-470-66677-7, John Wiley & Sons Ltd, Chichester, UK, 2011.

[11] G.-Y. Li, G.-J. Zhao, K.-L. Han, G.-Z. He, A TD-DFT study on the cyanide-chemosensing mechanism of 8-formyl-7-hydroxycoumarin, J. Comput. Chem., 32 (2011), 668-674.

[12] G.-J. Zhao, K.-L. Han, Hydrogen bonding in the electronic excited state, Acc. Chem. Res., 45 (2012), 404-413.

[13] T. L. Arbeloa, F. L. Arbeloa, M. J. Tapia, I. L. Arbeloa, Hydrogen-bonding effect on the photophysical properties of 7-aminocoumarin derivatives, J. Phys. Chem., 97 (1993), 4704-4707.

[14] R. Nakagaki, N. Kitamura, J. Aoyama, H. Ohtsubo, Hydrogen bonding of aromatic amines in hydroxylic solvents 2. Absorption and emission spectroscopy of substituted 7-aminocoumarins and 7-aminocarbostyrils, J. Photochem. Photobiol. A, 80 (1994), 113-119.

[15] P. M. Palmer, Y. Chen, M. R. Topp, Simple water clusters of coumarins 151 and 152A studied by IR-UV double resonance spectroscopy, Chem. Phys. Lett., 318 (2000), 440-447.

[16] T. G. Kim, M. R. Topp, Solvent effects on the fluorescence depolarization rates of coumarins in solution: the likely influence of site-selective hydrogen bonding, J. Phys. Chem. A, 108 (2004), 7653-7659.

[17] K. Das, B. Jain, H. S. Patel, Hydrogen bonding properties of coumarin 151, 500, and 35: the effect of substitution at the 7-amino position, J. Phys. Chem. A , 110 (2006), 1698-1704.

[18] E. T. J. Nibbering, F. Tschirschwitz, C. Chudoba, T. Elsaesser, Femtochemistry of hydrogen bonded complexes after electronic excitation in the liquid phase: the case of coumarin 102, J. Phys. Chem. A, 104 (2000), 4236-4246.

[19] S. Nad and H. Pal, Unusual photophysical properties of coumarin 151, J. Phys. Chem. A, 105 (2001), 1097-1106.

[20] H. Pal, S. Nad, M. Kumbhakar, Photophysical properties of coumarin 120: unusual behavior in nonpolar solvents, J. Chem. Phys., 119 (2003), 443-452.

[21] E. Pines, D. Pines, Y.-Z. Ma, G. R. Fleming, Femtosecond pump-probe measurements of solvation by hydrogen-bonding interactions, ChemPhysChem, 5 (2004), 1315-1327.

[22] E. T. J. Nibbering, H. Fidder, E. Pines, Ultrafast Chemistry: using time-resolved vibrational spectroscopy for interrogation of structural dynamics, Annu. Rev. Phys. Chem., 56 (2005), 337-367.

[23] E. Krystkowiak, K. Dobek, A. Maciejewski, Origin of the strong effect of protic solvents on the emission spectra, quantum yield of fluorescence and fluorescence lifetime of 4-aminophthalimide. Role of hydrogen bonds in deactivation of S_1-4-aminophthalimide, J. Photochem. Photobiol., A, 184 (2006), 250-264.

[24] N. P. Wells, M. J. McGrath, T. Siepmann, D. F. Underwood, D. A. Blanck, Excited state hydrogen bond dynamics: coumarin 102 in acetonitrile-water binary mixtures, J. Phys. Chem. A, 112 (2008), 2511-2514.

[25] E. Krystkowiak, K. Dobek, G. Burdziński, A. Maciejewski, Radiationless deactivation of 6-aminocoumarin from the S_1-ICT state in nonspecifically interacting solvents, Photochem. Photobiol. Sci., 11 (2012), 1322-1330.

[26] E. Krystkowiak, A. Maciejewski, Changes in energy of three types of hydrogen bonds upon excitation of aminocoumarins determined from absorption solvatochromic experiments, Phys. Chem. Chem. Phys., 13 (2011), 11317-11324.

[27] R. J. Cave, K. Burke, E. W. Castner, Jr., Theoretical investigation of the ground and excited states of coumarin 151 and coumarin 120, J. Phys. Chem. A, 106 (2002), 9294-9305.

[28] D. Jacquemin, E.A. Perpete, X. Assfeld, G. Scalmani, M.J. Frisch, C. Adamo, The geometries, absorption and fluorescence wavelengths of solvated fluorescent coumarins: a CIS and TD-DFT comparative study, Chem. Phys. Lett., 438 (2007), 208-212.

[29] R. Improta, V. Barone, G. Scanlmaini, M. J. Frisch, A state-specific polarizable continuum model time dependent density functional theory method for excited state calculations in solution, J. Chem. Phys., 125 (2006), 054103-054111.

[30] R. Improta, G. Scalmani, M. J. Frisch, V. Barone, Toward effective and reliable fluorescence energies in solution by a new state specific polarizable continuum model time dependent density functional theory approach, J. Chem. Phys., 127 (2007), 074504-074512.

[31] S. Bagheri, H.R. Masoodi, M. Mohammadi, M. Zakarianezhad, B. Makiabadi, The influence of number of nitrogen atoms on the NMR data in aromatic azine…HF complexes, Chem. Phys. Lett., 572 (2013), 26-31.

[32] W.-W. Zhao, Y.-H. Ding, Q.-Y. Xia, Time-dependent density functional theory study on the absorption spectrum of coumarin 102 and its hydrogen-bonded complexes, J. Comput. Chem., 32 (2011), 545-553.

[33] D. Jacquemin, E. A. Perpete, I. Ciofini, C. Adamo, Accurate simulation of optical properties in dyes, Acc. Chem. Res., 42 (2009), 326-334.

[34] J. Tomasi, B. Mennucci, R. Cammi, Quantum mechanical continuum solvation models, Chem. Rev., 105 (2005), 2999-3093.

[35] M. Cossi, N. Rega, G. Scalmani, V. Barone, Energies, structures, and electronic properties of molecules in solution with the C-PCM solvation model, J. Comput. Chem., 24 (2003), 669-681.

[36] M.J. Frisch, G.W. Trucks, H.B. Schlegel, G.E. Scuseria, M.A. Robb, J.R. Cheeseman, G. Scalmani, V. Barone, B. Mennucci, G.A. Petersson, H. Nakatsuji, M. Caricato, X. Li, H.P. Hrat-chian, A.F. Izmaylov, J. Bloino, G. Zheng, J.L. Sonnenberg, M. Hada, M. Ehara, K. Toyota, R. Fukuda, J. Hasegawa, M. Ishida, T. Nakajima, Y. Honda, O. Kitao, H. Nakai, T. Vreven, J.A. Montgomery Jr., J.E. Peralta, F. Ogliaro, M. Bearpark, J.J. Heyd, E. Brothers, K.N. Kudin, V.N. Staroverov, R. Kobayashi, J. Normand, K. Raghavachari, A. Rendell, J.C. Burant, S.S. Iyengar, J. Tomasi, M. Cossi, N. Rega, J.M. Millam, M. Klene, J.E. Knox, J.B. Cross, V. Bakken, C. Adamo, J. Jaramillo, R. Gomperts, R.E. Stratmann, O. Yazyev, A.J. Austin, R. Cammi, C. Pomelli, J.W. Ochterski, R.L. Martin, K. Morokuma,V.G.

Zakrzewski, G.A. Voth, P. Salvador, J.J. Dan-nenberg, S. Dapprich, A.D. Daniels, O. Farkas, J.B.Foresman, J.V. Ortiz, J. Cioslowskiand, D.J. Fox, Gaussian 09, Revision A02 (Gaussian Inc., Wallingford, CT, 2009).

[37] M. J. Kamlet, J. L. M. Abboud, M. H. Abraham, R. W. Taft, Linear solvation energy relationships. 23. A comprehensive collection of the solvatochromic parameters,π*, α and β , and some methods for simplifying the generalized solvatochromic equation, J. Org. Chem., 48 (1983), 2877-2887.

[38] Y. Marcus, M. J. Kamlet, R. W. Taft, Linear solvation energy relationships: standard molar Gibbs free energies and enthalpies of transfer of ions from water into nonaqueous solvents, J. Phys. Chem., 92 (1988), 3613-3622.